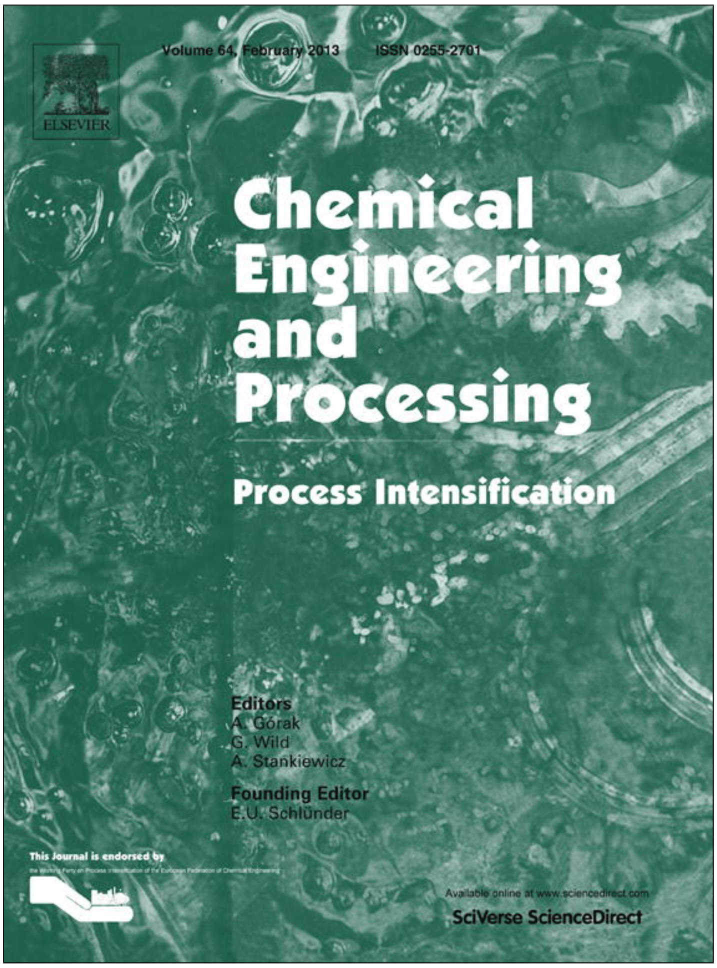
Volume 64, February 2013 ISSN 0255-2701
ELSEVIER
Chemical Engineering and Processing
Process Intensification
Editors
A. Górak
G. Wild
A. Stankiewicz
Founding Editor
E.U. Schlünder
This Journal is endorsed by
Available online at www.sciencedirect.com
SciVerse ScienceDirect

Chemical Engineering and Processing 64 (2013) 31–37

Contents lists available at SciVerse ScienceDirect

Chemical Engineering and Processing: Process Intensification

journal homepage: www.elsevier.com/locate/cep

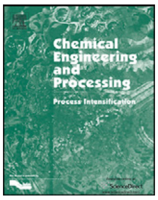

# Bio-ethanol steam reforming and autothermal reforming in 3-μm channels coated with RhPd/$CeO_2$ for hydrogen generation

Núria J. Divins[a,b], Eduardo López[a,c], Ángel Rodríguez[d], Didac Vega[d], Jordi Llorca[a,b,*]

[a] Institut de Tècniques Energètiques, Universitat Politècnica de Catalunya, Diagonal 647, Ed. ETSEIB, 08028 Barcelona, Spain
[b] Centre for Research in Nanoengineering, Universitat Politècnica de Catalunya, Pasqual i Vila 15, 08028 Barcelona, Spain
[c] Planta Piloto de Ingeniería Química (CONICET-UNS), Camino de la Carrindanga km7, 8000 Bahía Blanca, Argentina
[d] Departament d'Enginyeria Electrònica, Universitat Politècnica de Catalunya, Jordi Girona 1-3, 08034 Barcelona, Spain

ARTICLE INFO

*Article history:*
Received 8 March 2012
Received in revised form
20 September 2012
Accepted 21 October 2012
Available online 5 December 2012

*Keywords:*
Hydrogen
Microreactor
Silicon microchannel
Ethanol
Bio-ethanol
Steam reforming
Autothermal reforming

ABSTRACT

A silicon micromonolith of 7 mm diameter and 0.2 mm length containing 1.5 million regular channels with a diameter of 3.3 μm was used for obtaining hydrogen through ethanol or bio-ethanol steam reforming (ESR) and oxidative steam reforming (OSR). The microchannels were coated with RhPd/$CeO_2$ catalyst by a two-step method. First a $CeO_2$ layer of ca. 100 nm thickness was deposited from cerium methoxyethoxide over a $SiO_2$ layer, which was previously grown over the silicon microchannels by oxidation. Then, noble metals were grafted over the $CeO_2$ support from chloride precursors. The unit was successfully tested for hydrogen production, achieving hydrogen rates of $180\,L_{H_2}\,cm_R^{-3}$ for the steam reforming of bio-ethanol at 873 K, S/C = 2 and 0.009 s contact time. Reaction yields of 3.8 and 3.7 mol hydrogen generated per mol ethanol in feed were measured for ESR and OSR, respectively. A performance comparison was performed with a conventional cordierite monolith with the same catalyst formulation. Results show for the silicon microreactor an outstanding improvement of the specific hydrogen production rate, operating at considerably reduced residence times, due to the increase in contact area per unit volume.

## 1. Introduction

Motivated by fossil fuel depletion, harmful gas emissions from combustion engines, increasing world energy demand and non-homogeneous distribution of energy resources, hydrogen and fuel cells are receiving increasing attention as new tools for the management of energy. The catalytic steam reforming and oxidative steam reforming of renewable fuels derived from biomass has attracted much attention as an efficient technology for hydrogen production because it provides high yields at reasonable cost. Among several renewable fuels, the use of alcohols (i.e. methanol and ethanol) and dimethyl ether (DME) is attractive due to their availability, high volumetric energy density and easy transportation [1].

The range of applications of fuel cells spans from commercial stationary large power plants to automotive and other mobile devices as well as portable electronic gadgets requiring less than 1 W electrical output. Market analyses expect portable applications to enjoy widespread market success. This has moved researchers to investigate the development of miniaturized fuel cell systems, including reformers for the on-site generation of hydrogen [2]. At present, portable electronic devices show remarkably improved performances, which lead to greater consumptions of electrical power. Moreover, the tendency towards miniaturization and the wireless revolution is being restrained by battery life. Fuel cells last much longer than batteries and do not need to be replaced. However, fuel cell implementation in handheld electronics could be restrained if hydrogen feeding and/or refueling is not properly solved. Although considerable work has been performed on hydrogen production via reforming reactions using conventional reactors, the scale reduction required for this market renders their utilization impractical. Furthermore, reforming reactions show strong thermal effects and conventional fixed-bed reactors exhibit poor heat transfer characteristics. Microreactors assess both the problems of moving down the scale and increasing the heat transfer rate by the deposition of the catalyst directly on the reactor walls and the introduction of new manufacturing techniques which permit, along with the miniaturization involved, the achievement of remarkable increases in the specific contact area [3]. The small dimensions attained for microchannels and their high reproducibility allow for better reaction control by achieving previously inaccessible residence times, short diffusional distances and flow pattern homogeneity, resulting in a considerable decrease in the

---

[*] Corresponding author at: Institut de Tècniques Energètiques, Universitat Politècnica de Catalunya, Av. Diagonal 647, Ed. ETSEIB, 08028 Barcelona, Spain. Tel.: +34 93 401 17 08; fax: +34 93 401 71 49.
*E-mail address:* jordi.llorca@upc.edu (J. Llorca).

0255-2701/$ – see front matter © 2012 Elsevier B.V. All rights reserved.
http://dx.doi.org/10.1016/j.cep.2012.10.018

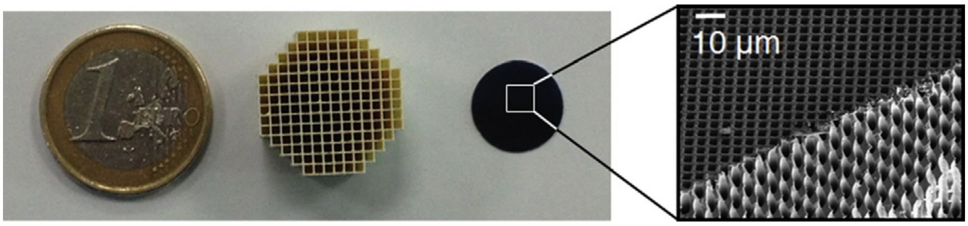

**Fig. 1.** Left: snapshot of the catalytic silicon micromonolith and the conventional cordierite monolith used in this work. Right: detail (SEM) of the silicon microchannels.

amount of catalyst required with respect to conventional reactors. Also, microreaction technology provides enhanced safe operation in the management of hydrogen-producing reactions because large volumes are avoided, permitting the use of process parameters of otherwise explosive regimes. Therefore, microreactors appear as an invaluable technology for boosting the implementation of on-site and on-demand generation of hydrogen for portable applications, thus avoiding limitations imposed by hydrogen storage.

Numerous micro-devices for the production of hydrogen from methanol steam reforming at 533–723 K have been reported [4], but the high temperatures required for the steam reforming of ethanol (ESR) has prevented extensive work in this field [5]. Men et al. from the Institute of Microtechnology Mainz (IMM) tested several catalyst formulations based on Ni, Rh, Co, and Ni–Rh for ESR in a microchannel reactor (channels 500 μm width and 250 μm depth) [6]. The best results were obtained over Ni–Rh/$CeO_2$, which showed no deactivation during a 100 h catalytic test at 923 K. Casanovas et al. from the Technical University of Catalonia (UPC) developed a microreactor for the generation of hydrogen from ethanol under an autothermal regime [7]. A two-sided platelet microreactor was designed for transferring the heat released during ethanol total catalytic oxidation over a $CuMnO_x$ catalyst in one side of the microreactor to the other side, where ESR occurred over a $CoO_x$–ZnO catalyst. Görke et al. from the Institute for Micro Process Engineering (Karlsruhe) used a microchannel reactor (channels 200 μm width and depth) to produce hydrogen by ESR over a Rh/$CeO_2$ catalyst [8]. For temperatures above 898 K, a space time yield four times higher than that obtained in conventional reactors was reached. Cai et al. from CNRS and the University of Lyon used a microreactor with channels 500 μm wide and deep, loaded with an Ir/$CeO_2$ catalyst, and hydrogen productivity was found significantly higher than in conventional fixed-bed reactors, essentially due to better heat and mass transfers [9]. These are pioneering examples reported in the open literature concerning the generation of hydrogen from ethanol using microreactor technologies. More recently, Peela et al. from the Indian Institute of Technology (IIT) performed steam reforming and oxidative steam reforming of ethanol over Rh/$CeO_2$/$Al_2O_3$ in a microreactor with channels 500 μm wide and 400 μm deep and showed that microchannels produced hydrogen without diffusional effects in the catalyst layer with respect to a packed bed reactor [10–12]. Domínguez et al. from UPC coated a plate microreactor with cobalt talc, $Co_3[Si_2O_5]_2(OH)_2$, and performed ESR at low temperature (648 K) with trace CO formation [13]. Rahman et al. from the Imperial College London used a catalytic hollow fiber microreactor loaded with a Ni/MgO–$CeO_2$ to carry out ESR, with a flow rate of hydrogen three fold higher than that obtained in a fixed-bed reactor [14,15]. Finally, Kolb et al. from IMM in collaboration with Rosetti Marino Company tested Rh–Ni and Rh–Co/$Al_2O_3$-based catalysts and designed the concept of a microstructured 50 kW ethanol fuel processor [16].

To further reduce the hydrogen generation scale while maintaining system efficiency can hardly be attained by using conventional geometries and/or manufacture techniques of present-day microreactors. Therefore, the development of breakthrough technologies capable to provide higher hydrogen generation rates per unit volume and, at the same time, enable downscaling is required. In that sense, we have reported a novel approach to minimize systems for hydrogen production by using silicon micromonoliths with millions of parallel microchannels per square centimeter with a diameter of only ~3–4 μm [17]. Such geometry is achieved through photo-assisted electrochemical etching in silicon wafers. The parallel channels show spectacular reproducibility, assuring excellent flow distribution (Fig. 1) if proper manifold geometry is provided. By means of precisely designed methods, the channel walls can be successfully coated with homogeneous thin layers of appropriate catalysts. With the resultant geometry, the specific contact area increases ca. 100 times with respect to conventional microreactors, reaching fabulous values of $10^6\ m^2\ m^{-3}$. A silicon micromonolith coated with a $Co_3O_4$/ZnO catalyst was tested successfully for ESR [18] and used to build up a complete ethanol processor with in-series units comprising a total of ca. $2 \times 10^7$ channels [19]. Specific production rates exceeding 3.2 $L_N$ of $H_2$ per mL of liquid fed and $cm^3$ of micromonolith under residence times of the order of milliseconds were possible due to the great geometric area of the micromonoliths. In addition to ESR, silicon micromonoliths coated with Au/$TiO_2$ were tested for CO preferential oxidation in the presence of excess hydrogen in order to simulate reformer outlet streams [20]. However, although inexpensive Co-based catalysts perform well for the ESR at low temperature in terms of activity and selectivity [21,22], they suffer from severe deactivation due to extensive carbon deposition [23]. A survey of the literature reveals that noble metal-based catalysts (Pd, Pt, Rh, Ru, Ir) perform well for ESR [24]. They are stable and exhibit high activity, provided that high enough temperature levels are selected for operation ($T > 873$ K). In this work, we report the use of the novel macroporous silicon substrate loaded with a stable, noble metal-based catalyst, RhPd/$CeO_2$, to produce hydrogen by ESR and OSR and intended to feed microfuel cells for portable devices. Both synthetic ethanol and bio-ethanol have been used.

## 2. Experimental

### 2.1. Silicon microreactor manufacture

Photoassisted electrochemical etching was performed over <1 0 0> *n*-type float-zone silicon. In the etching procedure, the prestructured silicon wafer (by lithography, square arrange) was in contact with the electrolyte, while the backside was illuminated through an array of LEDs with an 880-nm peak emission wavelength. A constant anodic potential of 2 V was applied. After the growing of the channels, the pores were opened from the back side by removing the remaining silicon with 25 wt% tetramethylammonium hydroxide (TMAH) solution at 358 K. The resulting structure was a silicon micromonolith (~0.2 mm length, Ø16 mm) with perfectly cylindrical channels opened at both sides and arranged in a square lattice with a periodicity of 4 μm. The micromonolith contained ca. $2 \times 10^6$ channels with a specific contact area of $4.1 \times 10^5\ m^2\ m^{-3}$ and an open frontal area of 34%. A pressure drop of only ca. 170 Pa with nitrogen flowing at 60 mL $min^{-1}$ at room temperature was measured for the micromonolithic structure, which is virtually identical to the value predicted by the Poiseuille law (165 Pa) [25].

### 2.2. Catalyst preparation

The silicon micromonolith was thermally treated at 1373 K under a dry $O_2$ atmosphere for 30 min to form a $SiO_2$ layer on the microchannel walls. The terminal hydroxyl groups of the $SiO_2$ layer were then exchanged at room temperature with cerium methoxyethoxide (Alfa Aesar), which was forced to pass through the microchannels by applying a pressure gradient of 75 kPa. A homogeneous and well-adhered layer of $CeO_2$ was obtained by thermal decomposition at 773 K for 6 h (5 K $min^{-1}$). Finally, noble metals (1%, w/w) were grafted onto the $CeO_2$ support by free impregnation by passing a water/acetone $PdCl_2/RhCl_3$ solution (Sigma–Aldrich) through the silicon microchannels coated with $CeO_2$. The resulting catalytic silicon micromonolith was dried at 393 K and calcined in air at 573 K for 6 h (2 K $min^{-1}$). The catalyst mass incorporated into the microchannels was ca. 3 mg.

For comparative purposes, a conventional 400 cpsi (Corning Celcor®) cordierite monolith as cylinder of 1.8 cm diameter and length was coated with the same $RhPd/CeO_2$ catalyst. The monolith was first coated with ca. 250 mg of cerium oxide by repetitive immersion in an aqueous solution of $Ce(NO_3)_2 \cdot 6H_2O$ (Fluka), followed by 2 h drying at 373 K under continuous rotation (60 rpm) and calcination at 773 K. Noble metals were then added in a single step by incipient wetness impregnation using a water/acetone $PdCl_2/RhCl_3$ solution (Sigma–Aldrich). The resulting catalytic monolith was dried at 373 K and calcined in air at 673 K.

### 2.3. Characterization methods

Scanning electron microscopy (SEM) was carried out on a Neon40 Crossbeam Station (Zeiss) equipped with a field emission (FE) gun. High-resolution SEM pictures were taken after cleaving the sample at different depths along the channels to see the homogeneity of pore infiltration. X-ray diffraction (XRD) measurements were performed with a Siemens D5000X diffractometer with Cu Kα incident radiation. XRD profiles were recorded from 3 to 75° ($2\theta$) at a step size of 0.02° and step time of 18 s.

### 2.4. Reaction tests

In order to evaluate the reaction performance of the functionalized silicon micromonolith, a disk of 8 mm in diameter was cut with a laser device and glued with epoxy into a stainless steel washer (OD 19 mm, ID 7 mm), which was subsequently sealed in a stainless steel housing inside a furnace (Carbolite, accuracy ±0.1 K). Several reaction experiments were conducted under both ESR and OSR conditions. Feed concentrations at realistic conditions were selected, using non-diluted ethanol/water and bio-ethanol/water liquid mixtures. The catalyst was treated prior to the experiments under flowing $H_2$ (20 mL $min^{-1}$, 10% in He) at 550 K for 60 min. Reaction mixtures consisting of water and ethanol (Panreac) or bioethanol (Bioetanol de la Mancha, S.L.; 5 ppm S, 1 ppm Cl, 0.4 ppm P) were introduced into the microreactor with a Knauer HPLC pump. For OSR experiments, different concentrations of $O_2$ were dosed by using an independent mass flow controller (M + W Instruments). The feed was passed at atmospheric pressure through the catalytic micromonolith at 4–86 STP mL $min^{-1}$, leading to a contact time of $2 \times 10^{-3}$–$3.6 \times 10^{-2}$ s. Conventional monoliths were tested in a similar way under the same reactant mixtures at 26–160 STP mL $min^{-1}$, resulting in a contact time of 2.4–14.5 s. Reaction products were analyzed online continuously with an Agilent 3000 A gas micro-chromatograph equipped with MS 5 Å, PlotU and Stabilwax columns. By measuring under steady-state conditions and in a precise period of time both the composition and flowrate of the gaseous outlet stream we verified the correct closure of the mass balance. Molar flowrates of $H_2$, CO, $CO_2$, $CH_4$ and $CH_3CHO$ in the reactor effluent were calculated using the chromatographic analyses and total volumetric flowrate data (only negligible amounts of acetone, ethane and ethylene were detected).

## 3. Results and discussion

### 3.1. Catalyst deposition

Given the small dimensions of the channels in the silicon micromonolith, we developed a method specifically designed for coating the microchannel walls with $RhPd/CeO_2$ catalyst without channel blocking, as detailed in Section 2.2. In order to facilitate the adherence of $CeO_2$ onto the silicon substrate, the silicon micromonolith was first oxidized to develop a thin $SiO_2$ layer of about 100 nm thickness. The hydroxyl groups attached to the surface of the oxide layer acted as anchoring sites and interacted with the cerium alkoxyde precursor ($Ce(O{-}CH_2{-}CH_2{-}O{-}CH_3)_4$) leading to the formation of a homogeneous $CeO_2$ layer upon calcination at 773 K. The synthesis was followed by X-ray diffraction (XRD) and scanning electron microscopy (SEM). Diffraction peaks at 28.6°, 33.1°, 47.5° and 56.3° in the XRD profile indicated the formation of the expected fcc $CeO_2$ structure. Rh and Pd were simultaneously deposited over the $CeO_2$ support by impregnation. Fig. 2 corresponds to scanning electron microscopy (SEM) images obtained directly on the resulting silicon micromonolith treated and functionalized with the method described and discussed above. A general profile view of adjacent microchannels after cutting the micromonolith is shown in Fig. 2a, and detailed images at higher magnification corresponding to the areas enclosed by black squares in Fig. 2a are depicted in Fig. 2b (profile view) and c (planar view). In Fig. 2b, the grey area corresponds to the silicon matrix, which is covered by a compact, homogeneous, and well-defined $SiO_2$ layer of about 100 nm thickness (black). Over the $SiO_2$ layer, a homogeneous and very uniform layer of $CeO_2$ is perfectly anchored (light grey), which is also about 100 nm thick. Very well-dispersed noble metal nanoparticles appear as bright dots over the $CeO_2$ support (Fig. 2a and c), most of them measuring <5 nm in size (Fig. 2c). Therefore, here we provide a well established methodology for coating silicon microchannels measuring a few micrometers in diameter with a thin layer of a ceria-based catalyst. We have already shown that other catalyst supports can be prepared by this method [17,20], thus opening the possibility of using such silicon microreactors for a wide range of reactions at the microscale.

### 3.2. Steam reforming tests

The overall reaction for ethanol steam reforming (Eq. (1)) yields 6 mol $H_2$ per mol of substrate (half of $H_2$ originates from water).

$$C_2H_5OH + 3H_2O \rightarrow 6H_2 + 2CO_2 \quad (1)$$

As already reported in the literature [24], the reaction scheme shown below (Eqs. (2)–(4)) summarizes the ethanol steam reforming process over $RhPd/CeO_2$ catalysts. First, ethanol decomposes into hydrogen, methane and carbon monoxide (Eq. (2)), followed by conventional methane steam reforming (MSR, Eq. (3)). The water-gas shift reaction (WGS, Eq. (4)) also occurs, consuming CO and rendering extra amounts of hydrogen. Both MSR and WGS are equilibrium-limited reactions.

$$C_2H_5OH \rightarrow CO + CH_4 + H_2 \quad (2)$$

$$CH_4 + H_2O \leftrightarrows CO + 3H_2 \quad (3)$$

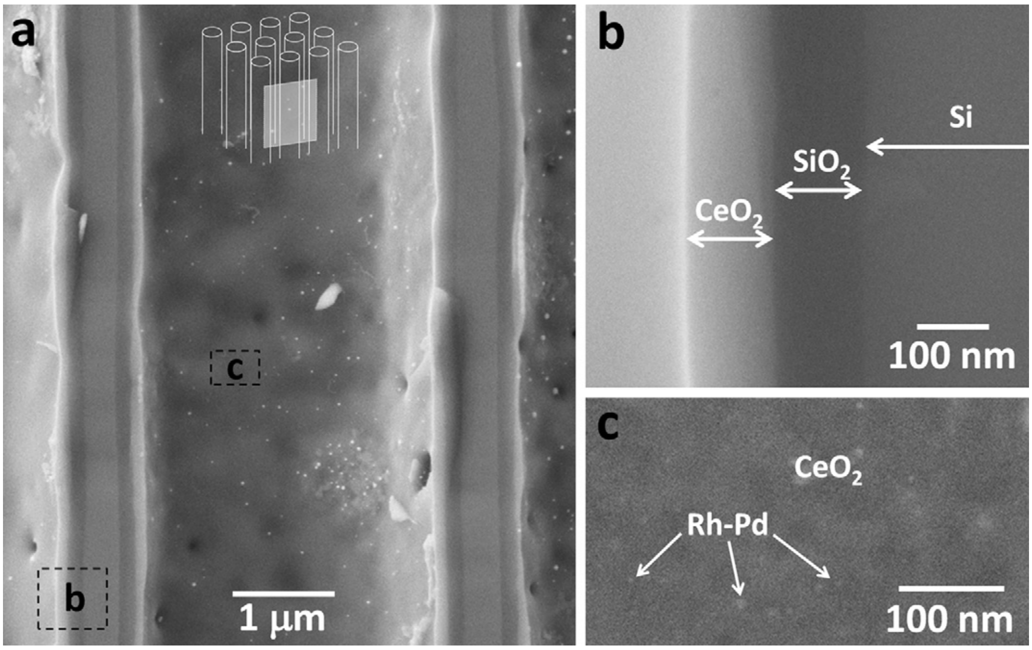

**Fig. 2.** Representative SEM image of the catalytic layer over a silicon microchannel as shown in the drawing (a); detail of a microchannel wall showing the $SiO_2$ and $CeO_2$ layers over the Si substrate (b); detail of the catalyst layer of $RhPd/CeO_2$ (c).

$$CO + H_2O \leftrightharpoons CO_2 + H_2 \tag{4}$$

ESR is highly endothermic, $\Delta H^\circ_{298\,K} = +347\,kJ\ mol^{-1}$. The energy balance of the production of hydrogen by steam reforming can be improved by using a combination of steam and oxygen (oxidative steam reforming) at the reactor inlet (Eq. (5)), which may approach an autothermal regime ($\Delta H^\circ \sim 0$), at the expense of hydrogen yield.

$$C_2H_5OH + (3-n)H_2O + n/2O_2 \rightarrow (6-n)H_2 + 2CO_2 \tag{5}$$

We selected in this contribution several parameters to quantify the reforming performance of the unit: ethanol conversion ($\chi_{EtOH}$), hydrogen selectivity, volumetric hydrogen production rate ($\dot{V}$) and hydrogen yield ($\theta_{H_2}$) as presented in Eqs. (6)–(9).

$$\chi_{EtOH} = \frac{F_{EtOH,reacted}}{F_{EtOH,feed}} \times 100 \tag{6}$$

$$S_{H_2} = \frac{F_{H_2}}{F_{H_2} + F_{CH_4} + F_{CO_2} + F_{CO} + F_{CH_3CHO}} \times 100 \tag{7}$$

$$\dot{V}_{H_2} = \dot{V}_{g,outlet} \cdot S_{H_2} \tag{8}$$

$$\theta_{H_2} = \frac{F_{H_2}}{6 \cdot F_{EtOH}} \tag{9}$$

Regarding Eq. (9), the factor 6 in the denominator is applied only in the cases where equal or higher than stoichiometric amounts of water are fed, i.e., in all SR experiments reported as well as in all OSR experiments operated at S/C = 2. In OSR tests with S/C = 1 in feed, the referred factor 6 in Eq. (9) should be replaced by a factor 5, as indicated by Eq. (5).

The steam reforming of synthetic ethanol was conducted for ethanol/water mixtures of S/C = 3 at temperatures ranging between 773 and 973 K. For a constant feed load (GHSV = 4.2 × $10^5$ $h^{-1}$), complete ethanol conversion was attained for $T > 873$ K (indicating the absence of by-passes and channels lacking catalyst). The influence of the residence time was also studied at 873 K for S/C = 3; the experiments were performed for 6 different space velocities comprised between GHSV = 2.1 × $10^5$ $h^{-1}$ and GHSV = 1.3 × $10^6$ $h^{-1}$, which correspond to residence times ($\tau$) between 3 and 17 milliseconds. Ethanol conversion, hydrogen yield, and selectivity values are reported in Fig. 3.

The ethanol conversion was almost complete for all the contact times tested, but the hydrogen yield decreased from 0.65 to 0.53 (Fig. 3a), due to the appearance of acetaldehyde at low contact times (acetaldehyde is produced by the dehydrogenation of ethanol). As shown in Fig. 3b, the selectivity values are close to equilibrium.

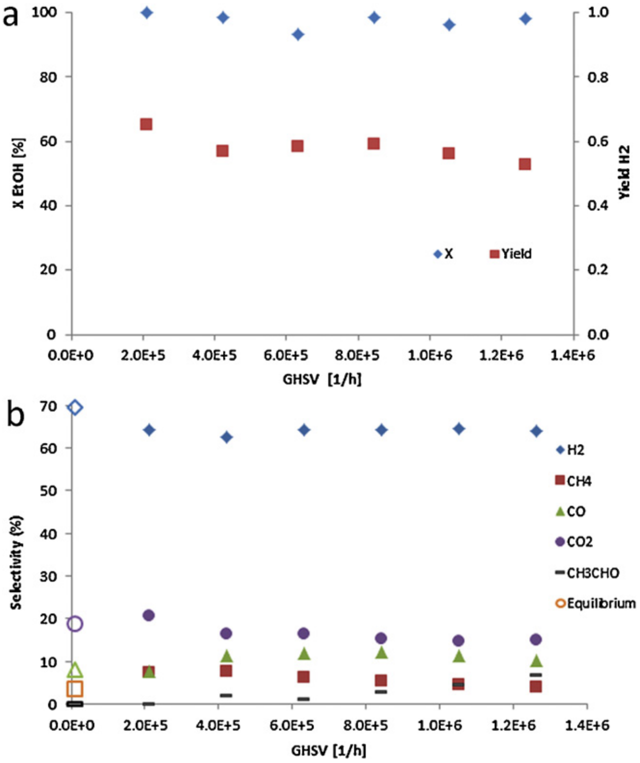

**Fig. 3.** Ethanol conversion and hydrogen yield (a) and selectivities (b) for ethanol steam reforming experiments. $T = 873$ K, $p = 1$ bar, S/C = 3.

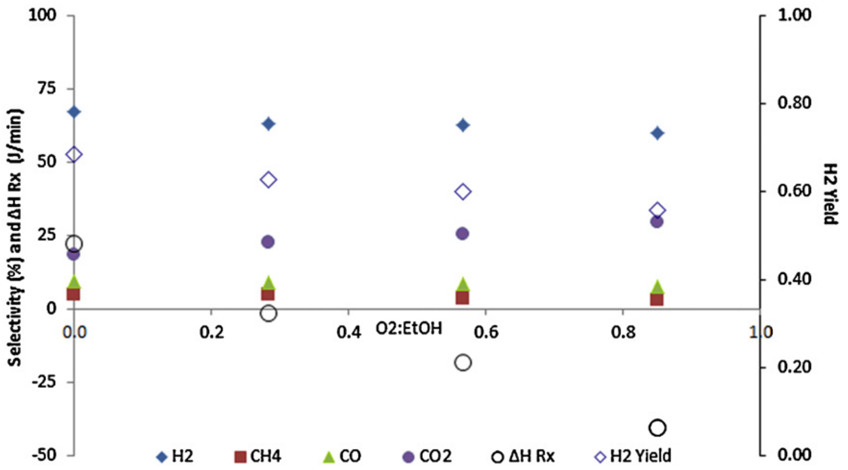

**Fig. 4.** Selectivities, reaction enthalpy and hydrogen yield for different $O_2$:EtOH in the oxidative steam reforming tests. $T = 873$ K, $p = 1$ bar, S/C = 2, GHSV = $3.8 \times 10^5$–$4.5 \times 10^5$ $h^{-1}$.

Reforming tests were also carried out with bio-ethanol/water mixtures of S/C = 2. This S/C ratio is closer to the stoichiometric value and represents severer reaction conditions. Nevertheless, 97% bio-ethanol conversion and 0.66 hydrogen yields were achieved at 873 K and 19 milliseconds residence time. The products distribution attained was $S_{H2} = 65.0\%$, $S_{CH4} = 6.9\%$, $S_{CO2} = 19.0\%$, $S_{CO} = 9.1\%$. Therefore, the values reached are very similar to those obtained with synthetic ethanol and also close to the equilibrium.

### 3.3. Oxidative steam reforming tests

Regarding the ethanol OSR performance, we studied the influence of the oxygen/ethanol ratio at 873 K and S/C = 2, as reported in Fig. 4. When higher amounts of oxygen were dosed while keeping constant the liquid feed, hydrogen, methane and carbon monoxide decreased as expected, leading to an increase of carbon dioxide. No acetaldehyde was detected for all the tests. The hydrogen yield diminished as well, decreasing from 0.68 for ESR conditions to 0.56 for $O_2$:EtOH = 0.85. Nevertheless, the energy balance is highly improved when oxygen is present in the reactor feed, as shown in Fig. 4. ATR operating conditions can be achieved for $O_2$:EtOH = 0.28. For large oxygen/ethanol values, the reaction becomes intensely exothermic at the expense of excessive hydrogen losses, rendering its use economically unfeasible. As reported elsewhere [26,27], oxygen/ethanol ratios between 0.3 and 0.6 appear the most appropriate in order to obtain conveniently high hydrogen yields and slightly exothermic operating conditions.

Oxidative steam reforming tests were also performed at 873 K reducing the amount of water in feed to S/C = 1. The hydrogen selectivities decreased 2% on average when compared to experiments with S/C = 2. A slight diminution in the moles of hydrogen generated per mol ethanol in feed is also measured, indicating poorer reforming conditions. In fact, higher amounts of water shift the equilibria of MSR and WGS to the right (see Eqs. (3) and (4)). Additionally, because less water is present in the reaction medium the probability of coke deposition increases, with the consequence of catalyst blocking and deactivation. On the other hand, mixtures with lower S/C, for the same amount of liquid fed, have more ethanol available and higher volumetric hydrogen production rates are measured for the operating temperatures selected here. Finally, the energetic cost of preheating and evaporating the surplus water when over-stoichiometric S/C are chosen should be considered in conjunction with the conclusions arising from the reaction performance for the final selection of the optimum operational S/C value.

The effect of impurities in bio-ethanol on the performance of OSR was tested as well. The S/C and $O_2$:EtOH were fixed to 2 and 0.5 (GHSV = $2.1 \times 10^5$ $h^{-1}$), respectively, and the temperature ranged between 773 and 873 K. At 873 K full ethanol conversion was attained and the distribution of products was: $S_{H2} = 60.4\%$, $S_{CO2} = 25.3\%$, $S_{CO} = 9.3\%$, $S_{CH4} = 4.9\%$ and $S_{CH3CHO} = 0.1\%$. After ca. 80 h of operation, no deactivation of the catalyst was observed.

### 3.4. Performance comparison with conventional monoliths

When a comparison of the performance between the silicon micromonolith and the conventional monolithic catalysts (400 cpsi) is intended, the inclusion of some kind of intensive measurement appears appropriate to equalize the obvious use of not completely similar operating conditions given the ca. 3 order of magnitude differences in the dimensions of the systems. In these terms, the specific hydrogen production rate ($V_{H_2}^{sp}$) normalizes volumetric hydrogen production rate by the volume of support and the ethanol injection load:

$$V_{H_2}^{sp}\left[\frac{\mathrm{Nml}_{H_2,g}}{\mathrm{ml}_{l,EtOH\times cm_R^3}}\right]=\frac{V_{H_2}[\mathrm{Nml}_{H_2},\mathrm{g/min}]}{V_{l,EtOH}[\mathrm{ml}_{l,EtOH}/\mathrm{min}]\cdot V_R[\mathrm{cm}_R^3]} \qquad (10)$$

Fig. 5 presents a comparison of the ESR performance between the silicon micromonolith and the conventional cordierite monolith using both the same catalytic formulation, namely, Pd–Rh/$CeO_2$. For the operating conditions selected for these experiments both reaction systems showed complete ethanol conversion and similar hydrogen yield. The dramatically superior contact area available in the silicon structure when compared to the cordierite monolith ($4.1 \times 10^5$ vs. $2.2 \times 10^3$ $m^2\,m^{-3}$, respectively) allows achieving similar hydrogen yields although residence times were reduced from $\tau \approx 5.3$ s to $\tau \approx 9 \times 10^{-3}$ s, as shown in Fig. 5. Very similar hydrogen and methane selectivities were measured as well. The operation of the silicon micromonolithic system at residence times in the order of milliseconds yields higher amounts of carbon monoxide in detriment of $CO_2$ when compared with the conventional monolith. In fact, as described elsewhere [24], the water gas shift reaction (Eq. (4)) occurs in-series with the ethanol decomposition and methane reforming reactions (Eqs. (2) and (3), respectively). Consequently, extremely reduced residence time ($\tau$) reduces the contribution of the water gas shift reaction. At the operating conditions of Fig. 5, equilibrium selectivities are 69.5%, 3.5%, 8.1% and 18.9%, for $H_2$, $CH_4$, CO and $CO_2$, respectively. Specific hydrogen

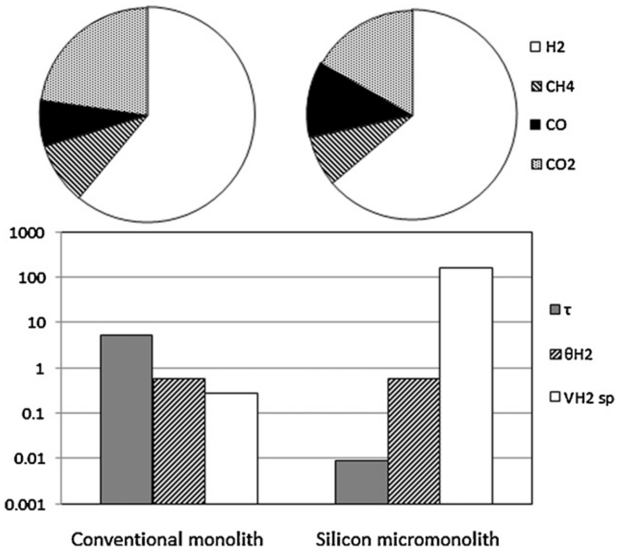

**Fig. 5.** Performance comparison of ethanol steam reforming over $PdRh/CeO_2$ in conventional $4 \times 10^2$ cpsi cordierite monoliths (left) and $2.6 \times 10^7$ cpsi silicon micromonoliths (right). $T = 873$ K, $p = 1$ bar, $x_{EtOH} = 100\%$, S/C = 3. Conventional monolith: $V_l = 0.055$ $mL_l$ $min^{-1}$, Si-micromonolith: $V_l = 0.021$ $mL_l$ $min^{-1}$.

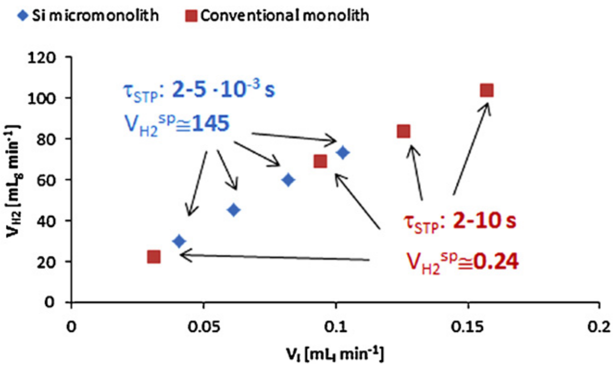

**Fig. 6.** Hydrogen production rates (both total and specific) and STP residence times for ethanol oxidative steam reforming for different liquid feed flow rates. Both the performance of the silicon micromonolith and of the conventional cordierite monolith are included. $T = 923$ K, $p = 1$ bar, $x_{EtOH} = 100\%$, S/C = 1, O/C = 0.526.

production rates are also reported in Fig. 5. As seen, a noticeable 580-fold increase of $V_{H_2}^{sp}$ was measured for the Si-micromonolith when compared with the cordierite monolith. If $V_{H_2}^{sp}$ is multiplied by the reactor volume for each system, then a similar value of ca. 1.3 $_{N}L_{H_2,g}/mL_{l,EtOH}$ is found in agreement with the measurement of almost the same hydrogen yield of 0.57 for both supports, as already mentioned.

Fig. 6 reports experimental results concerning oxidative steam reforming of ethanol in both the silicon micromonolith and the conventional cordierite monolith for different liquid feed loads. Both the S/C and O/C ratios in feed are kept constant through the experiments in Fig. 6 at 1 and 0.53, respectively. Again, operation at highly reduced residence times while achieving complete ethanol conversion and hydrogen yields of 0.58–0.61 (same as for the cordierite monolith) are possible for the silicon structure due to the 2 orders of magnitude increased contact area. Remarkable uniformity in the products selectivities were observed for OSR experiments, with almost no variation for the different loads and catalyst supports. Both reaction systems showed robustness facing the assayed load increase as shown in Fig. 6.

## 4. Conclusion

A monolithic silicon microreactor containing ca. $2 \times 10^6$ cylindrical channels of 3.3 μm diameter has been coated with $RhPd/CeO_2$ catalyst and successfully implemented for hydrogen production via ethanol steam reforming and oxidative steam reforming towards portable fuel cell feeding. An effective methodology for coating silicon microchannels with a thin, homogeneous, and well-adhered $RhPd/CeO_2$ catalyst layer has been developed. Reaction experiments have shown that Si microchannels loaded with $RhPd/CeO_2$ prove adequate to conduct both ethanol and bio-ethanol steam reforming and oxidative steam reforming. Complete ethanol conversion has been attained at $T > 873$ K for residence times of few milliseconds with excellent selectivity values. $H_2$ production rates exceeding 1.5 and 1.4 $L_N$ of $H_2$ per mL of liquid bio-ethanol fed were achieved under ESR and EOSR conditions, respectively. Activity values normalized per reactor volume amount to about 2 orders of magnitude higher when compared to operation with conventional 400 cpsi cordierite monoliths. Specific production rates exceeding 190 $L_N$ of $H_2$ per $cm^3$ of micromonolith were possible due to the great geometric area of the substrate. This novel concept represents a landmark in miniaturization technology in general and in micro-scale energy production in particular.

## Acknowledgements

This work has been carried out with the support of MICINN project CTQ2009-12520 and MINECO project ENE2012-36368. N.J.D. is grateful to UPC for a PhD grant. J.L. acknowledges ICREA Academia program.

## References

[1] C. Ledesma, M. Domínguez, N. Jiménez, E. López, J. Llorca, Hydrogen generation from renewables steam reforming of ethanol and dimethyl ether over structured catalysts, Chemistry Today 27 (2009) 40.
[2] G. Kolb, Fuel Processing for Fuel Cells, Wiley-VCH, Weinheim, 2008.
[3] W. Ehrfeld, V. Hessel, H. Löwe, Microreactors: New Technology for Modern Chemistry, Wiley-VCH, Weinheim, 2000.
[4] D.R. Palo, R.A. Dagle, J.D. Holladay, Methanol steam reforming for hydrogen production, Chemical Reviews 107 (2007) 3992.
[5] J. Llorca, Microreactors for the generation of hydrogen from ethanol, in: W.H. Lee, W.H. Lee (Eds.), Handbook of Sustainable Energy, Nova Science Publishers, Hauppauge, 2010, pp. 693–699 (Chapter 22).
[6] Y. Men, G. Kolb, R. Zapf, V. Hessel, H. Löwe, Ethanol steam reforming in a microchannel reactor, Process Safety and Environmental Protection 85 (2007) 413.
[7] A. Casanovas, M. Saint-Gerons, F. Griffon, J. Llorca, Autothermal generation of hydrogen from ethanol in a microreactor, International Journal of Hydrogen Energy 33 (2008) 1827.
[8] O. Görke, P. Pfeifer, K. Schubert, Kinetic study of ethanol reforming in a microreactor, Applied Catalysis A: General 360 (2009) 232.
[9] W. Cai, F. Wang, A. van Veen, C. Descorme, Y. Schuurman, W. Shen, C. Mirodatos, Hydrogen production from ethanol steam reforming in a micro-channel reactor, International Journal of Hydrogen Energy 35 (2010) 1152.
[10] N.R. Peela, D. Kunzru, Steam reforming of ethanol in a microchannel reactor: kinetic study and reactor simulation, Industrial and Engineering Chemistry Research 50 (2011) 12881.
[11] N.R. Peela, D. Kunzru, Oxidative steam reforming of ethanol over Rh based catalysts in a micro-channel reactor, International Journal of Hydrogen Energy 36 (2011) 3384.
[12] N.R. Peela, A. Mubayi, D. Kunzru, Steam reforming of ethanol over $Rh/CeO_2/Al_2O_3$ catalysts in a microchannel reactor, Chemical Engineering Journal 167 (2011) 578.
[13] M. Domínguez, G. Cristiano, E. López, J. Llorca, Ethanol steam reforming over cobalt talc in a plate microreactor, Chemical Engineering Journal 176–177 (2011) 280.
[14] M.A. Rahman, F.R. García-García, K. Li, On-board $H_2$ generation by a catalytic hollow fibre microreactor for portable device applications, Catalysis Communications 16 (2011) 128.
[15] M.A. Rahman, F.R. García-García, K. Li, Development of a catalytic hollow fibre membrane microreactor as a microreformer unit for automotive application, Journal of Membrane Science 390–391 (2012) 68.
[16] G. Kolb, Y. Men, K.P. Schelhaas, D. Tiemann, R. Zapf, J. Wilhelm, Development work on a microstructured 50 kW ethanol fuel processor for a small-scale

stationary hydrogen supply system, Industrial and Engineering Chemistry Research 50 (2011) 2554.

[17] J. Llorca, A. Casanovas, T. Trifonov, A. Rodriguez, R. Alcubilla, First use of macroporous silicon loaded with catalyst film for a chemical reaction: a microreformer for producing hydrogen from ethanol steam reforming, Journal of Catalysis 255 (2008) 228.

[18] A. Casanovas, M. Domínguez, C. Ledesma, E. Lopez, J. Llorca, Catalytic walls and micro-devices for generating hydrogen by low temperature steam reforming of ethanol, Catalysis Today 143 (2009) 32.

[19] E. López, A. Irigoyen, T. Trifonov, A. Rodríguez, J. Llorca, A million-channel reformer on a fingertip: moving down the scale in hydrogen production, International Journal of Hydrogen Energy 35 (2010) 3472.

[20] N.J. Divins, E. López, M. Roig, T. Trifonov, A. Rodríguez, F. González de Rivera, L.I. Rodríguez, M. Seco, O. Rossell, Llorca J, A million-channel CO-PrOx microreactor on a fingertip for fuel cell application, Chemical Engineering Journal 167 (2010) 597.

[21] J.A. Torres, J. Llorca, A. Casanovas, M. Domínguez, J. Salvadó, D. Montané, Steam reforming of ethanol at moderate temperature: multifactorial design analysis of Ni/$La_2O_3$–$Al_2O_3$, and Fe- and Mn-promoted Co/ZnO catalysts, Journal of Power Sources 169 (2007) 158.

[22] A. Casanovas, C. de Leitenburg, A. Trovarelli, J. Llorca, Catalytic monoliths for ethanol steam reforming, Catalysis Today 138 (2008) 187.

[23] M. Domínguez, E. Taboada, H. Idriss, E. Molins, J. Llorca, Fast and efficient hydrogen generation catalyzed by cobalt talc nanolayers dispersed in silica aerogel, Journal of Materials Chemistry 20 (2010) 4875.

[24] H. Idriss, M. Scott, J. Llorca, S.C. Chan, W. Chiu, P.Y. Sheng, A. Yee, M.A. Blackford, S.J. Pas, A.J. Hill, F.M. Alamgir, R. Rettew, C. Petersburg, S. Senanayake, M.A. Barteau, A phenomenological study of the metal/oxide interface, the role of catalysis in hydrogen production from renewable sources, ChemSusChem 1.11 (2008) 905.

[25] S. Roy, R. Raju, Modeling gas flow through microchannels and nanopores, Journal of Applied Physics 93 (2003) 4870.

[26] S. de Lima, A. da Silva, L. da Costa, U. Grahamb, G. Jacobs, B. Davis, L. Mattos, F. Noronha, Study of catalyst deactivation and reaction mechanism of steam reforming, partial oxidation, and oxidative steam reforming of ethanol over Co/$CeO_2$ catalyst, Journal of Catalysis 268 (2009) 268.

[27] W. Cai, F. Wang, E. Zhan, A.C. Van Veen, C. Mirodatos, W. Shen, Hydrogen production from ethanol over Ir/$CeO_2$ catalysts: a comparative study of steam reforming, partial oxidation and oxidative steam reforming, Journal of Catalysis 257 (2008) 96.